Cerebral Cortex August 2009;19:1937–1951
doi:10.1093/cercor/bhn220
Advance Access publication December 10, 2008

Differential Expression Patterns of *occ1*-Related Genes in Adult Monkey Visual Cortex

Toru Takahata[1,3], Yusuke Komatsu[1], Akiya Watakabe[1], Tsutomu Hashikawa[2], Shiro Tochitani[1,4] and Tetsuo Yamamori[1]

[1]Division of Brain Biology, National Institute for Basic Biology, Okazaki, Aichi 444-8585, Japan, [2]Laboratory for Neural Architecture, Brain Science Institute, RIKEN, Wako, Saitama 351-0198, Japan, [3]Department of Psychology, Vanderbilt University, Nashville, TN 37240, USA and [4]Department of Anatomy and Developmental Neurobiology, Institute of Health Biosciences, The University of Tokushima Graduate School, Tokushima 770-8501, Japan

We have previously revealed that *occ1* is preferentially expressed in the primary visual area (V1) of the monkey neocortex. In our attempt to identify more area-selective genes in the macaque neocortex, we found that *testican-1*, an *occ1*-related gene, and its family members also exhibit characteristic expression patterns along the visual pathway. The expression levels of *testican-1* and *testican-2* mRNAs as well as that of *occ1* mRNA start of high in V1, progressively decrease along the ventral visual pathway, and end of low in the temporal areas. Complementary to them, the neuronal expression of *SPARC* mRNA is abundant in the association areas and scarce in V1. Whereas *occ1*, *testican-1*, and *testican-2* mRNAs are preferentially distributed in thalamorecipient layers including "blobs," *SPARC* mRNA expression avoids these layers. Neither *SC1* nor *testican-3* mRNA expression is selective to particular areas, but *SC1* mRNA is abundantly observed in blobs. The expressions of *occ1*, *testican-1*, *testican-2*, and *SC1* mRNA were downregulated after monocular tetrodotoxin injection. These results resonate with previous works on chemical and functional gradients along the primate occipitotemporal visual pathway and raise the possibility that these gradients and functional architecture may be related to the visual activity–dependent expression of these extracellular matrix glycoproteins.

Keywords: extracellular matrix, follistatin-related protein/TSC-36/FSTL1, in situ hybridization, monocular deprivation, RLCS

Introduction

Recent genome-wide analysis of gene expression patterns in the mouse brain has unveiled the variety of genes that are expressed in distinct parcellation of neuronal anatomical architecture (Lein et al. 2007). It has been suggested that these genes play roles in the formation or function of such structure (Pimenta et al. 1995; Job and Tan 2003; Hamasaki et al. 2004).

Our own effort to identify area-selective genes in the adult monkey neocortex by differential display analysis has demonstrated that *occ1* mRNA is preferentially expressed in the primary visual area (V1) (Tochitani et al. 2001). Examination of the *occ1* mRNA expression by in situ hybridization (ISH) revealed the following anatomical features: *occ1* mRNA expression 1) is dependent on neuronal activity, 2) is preferentially localized in thalamorecipient layers including "blobs" in layers II/III, and 3) is also localized in thalamorecipient layers of the extrastriate, somatosensory, and auditory cortices, although the expression levels are much lower than that in V1. These characteristics are restricted to the expression in excitatory neurons, whereas the expression is activity independent in parvalbumin (PV)-containing γ-aminobutyric acidergic (GABAergic) inhibitory interneurons that are broadly distributed throughout the neocortex (Tochitani et al. 2001; Komatsu et al. 2005; Takahata et al. 2006).

Our continued analysis is to search for area-selective genes using restriction landmark cDNA scanning (RLCS) technique, a large-scale analysis of differential gene expression. By this means, we identified *testican-1* as a V1-enriched gene (Fig. 1*A*). The domain structure of the gene product of *testican-1* is closely related to that of *occ1*. Both are characterized by the presence of one follistatin domain (FS domain) followed by one extracellular calcium-binding domain (EC domain). At least 4 other genes are known to belong to this family (Yan and Sage 1999) (Fig. 1*B*). They are secreted glycoproteins and are considered as part of the extracellular matrix (ECM). Although their roles in anticell proliferation and anticell adhesion have been reported (Yan and Sage 1999), the physiological roles of those genes in the central nervous system remain to be elucidated. Recent studies suggest that the ECM is involved in the maturation and plasticity of the synapse (Pizzorusso et al. 2002; Dityatev and Schachner 2006). Thus, *occ1*-related genes may have significant roles in regulating synaptic plasticity in the visual area in the primate neocortex.

Here, we performed a comprehensive expression analysis of the members of this family, namely, *testican-1*, *testican-2*, *testican-3* (also referred to as *SPOCK*s), *secreted protein acidic and rich in cystein* (*SPARC*: also referred to as *BM-40* or *osteonectin*), and *SPARC-like1* (*SC1*: also referred to as *hevin*). We found both similar and complementary expression patterns of the members of this family to that of *occ1* in terms of area difference, particularly the V1-temporal association area (TE) gradient, lamina preference, blob preference, cell-type specificity, and sensory input dependence.

Materials and Methods

Animals and Sample Preparation

For RLCS analysis and quantitative real-time reverse transcriptase–polymerase chain reaction (RT-PCR), postmortem brain tissues of African green monkeys (*Cercopithecus aethiops*) were obtained from the Japan Poliomyelitis Research Institute and processed as previously described (Watakabe et al. 2001). For ISH, ten Japanese macaque monkeys (*Macaca fuscata*, adult, either sex, 2.9–9.1 kg) were used. Six of the Japanese macaques were subjected to monocular deprivation (MD) during 5–21 days before sacrifice as follows: 10 μl of tetrodotoxin (4.7 mM in saline) was slowly microinjected into the left eyeball twice a week under ketamine anesthesia. The pupil of the injected eye was dilated after operation. A part of these samples were used in our previous studies (Tochitani et al. 2001; Takahata et al. 2006). Four of the 6 MD samples (5, 10, 14, and 21 days MD each) were used for quantification of MD effect on gene expression (Fig. 9). All the animals were administered an overdose of pentobarbital (at least 100 mg/kg

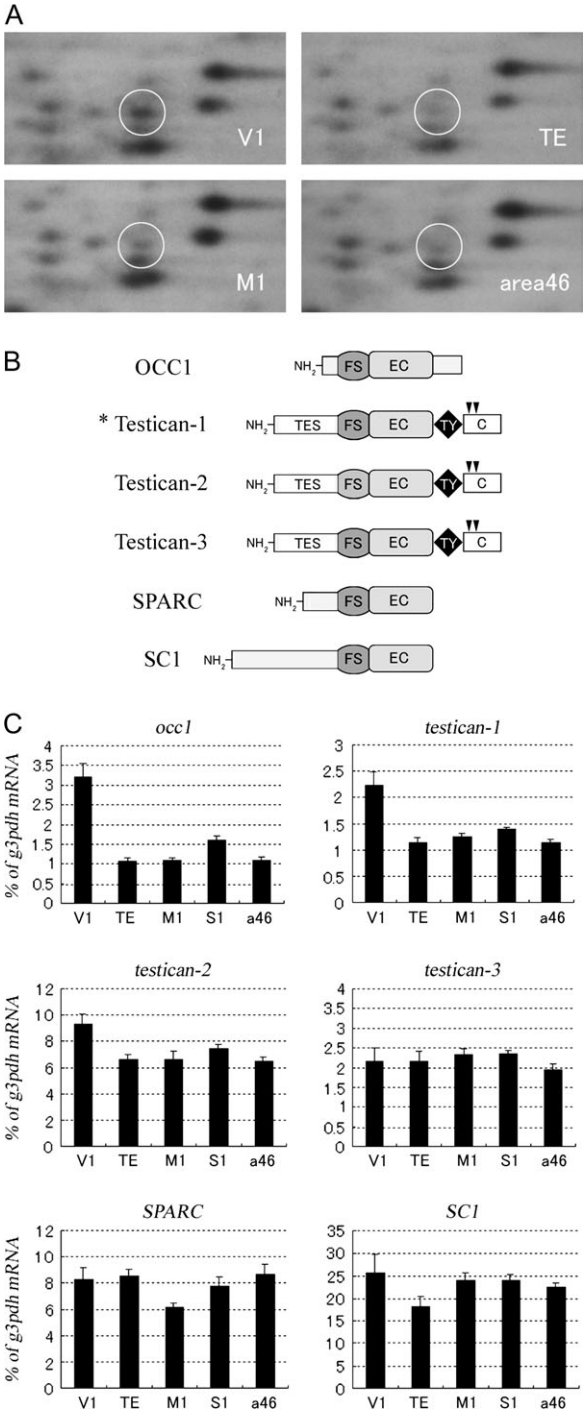

Figure 1. (*A*) The 2D electrophoresis in RLCS analysis in V1, TE, M1, and area 46. A more intense spot of the testican-1 gene was observed in V1 than in the other 3 areas (shown by a circle). (*B*) Schematic domain structures of occ1-related proteins. Testican-1 (*), which was identified as a V1-enriched gene, has a domain structure partially homologous to this group of proteins. They are characterized by one FS domain (FS) and a following EC domain (EC). Testicans have their unique domain both in the N-terminal (TES) and the C-terminal (C). TY denotes a thyroglobulin-like domain. Black arrowheads indicate the site of the glycosylated serine in Testicans (Alliel et al. 1993). SPARC has the highest homology to SC1 (ca. 70%) (Soderling et al. 1997). Open bars represent unidentified unique domains for each protein (Maurer et al. 1995). (*C*) Quantification of area difference in mRNA expression of occ1-related genes among V1, TE, M1, S1, and area 46 by real-time RT-PCR analysis. The amount of each mRNA was normalized as a ratio to the amount of the internal standard, g3pdh mRNA. occ1, testican-1, and testican-2 mRNAs were most abundant in V1 among these 5 areas.

body weight) and perfused intracardially with 4% paraformaldehyde (PFA) in 0.1 M phosphate buffer (PB). The brain was then removed from the skull, postfixed for 3–6 h at room temperature in the same fixative, cut into several blocks, and cryoprotected in 30% sucrose in 0.1 M PB at 4 °C. The block samples were frozen and stored at –80 °C. The frozen blocks were cut on a sliding microtome into 15-μm thick sections for fluorescence ISH or into 35-μm thick sections for colorimetric ISH and immunohistochemistry (IHC). The sections were maintained in a cryoprotectant solution (30% glycerol, 30% ethylene glycol, 40% 0.1 M phosphate-buffered saline [PBS]) at –30 °C until further processing when not used within 24 h after sectioning.

The protocols used in this study were approved by the Animal Research Committee of the National Institute for Basic Biology (NIBB) and the National Institute for Physiological Science, Japan; they were in accordance with the animal care guidelines of the National Institutes of Health, United States.

RLCS

Differential gene expression among 4 cortical areas (V1, TE, the primary motor area [M1], and Brodmann's area 46) of African green monkey was comprehensively identified by RLCS method as previously described (Suzuki et al. 1996; Shintani et al. 2004). Total RNAs were extracted separately from the cortical areas as described previously (Watakabe et al. 2001). Poly $(A)^+$ RNA was purified with BioMag Oligo $(dT)_{20}$ (PerSeptive Biosystems, Framingham, MA) following manufacturer's instructions. Double-stranded cDNAs were synthesized with an anchor primer targeting poly $(A)^+$ tail and SuperScript Choice System (Invitrogen, Carlsbad, CA). An overhang was created at the 5′-terminal of the cDNA using ApaLI, and the restriction cut site was radiolabeled by a full up reaction with [α-^{32}P] deoxynucleotides. Labeled fragments containing the 3′-terminal were collected using Dynabeads Oligo $(dT)_{25}$ (Dynal, Oslo, Norway) and cut away from the 3′-terminal by NotI digestion. The fragments were then subjected to agarose gel electrophoresis. After electrophoresis, the cDNA fragments in gel were digested with HinfI, in situ, and then subjected to acrylamide-gel electrophoresis. The cDNA fragments labeled and separated by the 2-dimensional (2D) electrophoresis were displayed as spots on X-ray films.

The spot intensity was carefully compared among the 4 cortical areas and the DNA fragments corresponding to the differential spot were eluted from the cutout gel and ligated with 2 adapters; one for the overhang site of ApaLI digestion and the other for the overhang site of HinfI digestion, and the ligated fragments were amplified by polymerase chain reaction (PCR) using the adapter sequence. The amplified fragments were cloned as described previously (Komatsu et al. 2005).

A total of 30 colonies per one cloned spot were picked up and subjected to PCR using the plasmid vector sequence. To select a positive clone corresponding to a differential spot, the fragments were subjected to restriction fragment length polymorphism (RFLP) analysis using a 4-base cutter, AluI. The inserted sequence that showed the most frequent pattern in RFLP was determined for each spot.

Real-Time RT-PCR

To quantify the difference in the mRNA expression levels among areas, real-time RT-PCR was performed. Total RNA was isolated from tissues of 5 cortical areas; V1, TE, M1, the primary somatosensory area (S1), and area 46. In all, 20 μg of each was subjected to RNase-free DNase treatment, followed by another round of acid guanidinium thiocyanate–phenol–chloroform extraction to completely remove the contaminating genomic DNA. Two micrograms of such RNA was converted to cDNA using random nonamer and MMLV reverse transcriptase (Invitrogen) and used as the template for real-time RT-PCR. Prepared cDNAs were reacted with specific primers for each gene (Supplementary Table 1) and SYBR Premix Ex Taq (Takara, Otsu, Japan) under the control of OPTICON2 (Bio-Rad, Hercules, CA). Only single bands were obtained when each reacted sample was electrophoresed, and the sequences of those bands were confirmed as derived from the targeted sequences of each gene. Lines of diluted solutions of brain samples were examined to determine amplification efficiencies for each primer set. The amount of each mRNA in each area was calculated by cycle

numbers, fluorescence intensities, and amplification efficiencies. The amount of each mRNA was expressed as the ratio to that of the *glyceraldehyde 3-phosphate dehydrogenase (g3pdh)* mRNA, which was used as an internal standard.

ISH

For colorimetric ISH, digoxigenin (DIG)-labeled antisense and sense riboprobes were prepared using a DIG-dUTP labeling kit (Roche Diagnostics, Indianapolis, IN). Riboprobes were newly prepared from the cDNA library of each animal by RT-PCR and conventional TA cloning techniques. The primer sequences are listed in Supplementary Table 1. The sense probes did not detect signals stronger than the background signal (data not shown). ISH was carried out as described previously (Tochitani et al. 2001; Takahata et al. 2006). Briefly, free-floating sections were soaked in 4% PFA/0.1 M PB (pH 7.4) overnight at 4 °C and treated with 10 μg/ml proteinase K for 30 min at 37 °C. After acetylation, the sections were incubated in the hybridization buffer (5× standard saline citrate [SSC; 1× means 150 mM NaCl, 15 mM Na citrate, pH 7.0], 50% formamide, 2% blocking reagent, 0.1% *N*-lauroylsarcosine [NLS], 0.1% sodium dodecyl sulfate, 20 mM maleic acid buffer; pH 7.5) containing 1.0 μg/ml DIG-labeled riboprobe at 60 °C overnight. Hybridized sections were washed by successively immersing in the washing buffer (2× SSC, 50% formamide, 0.1% NLS; 60 °C, 20 min, twice), RNase A buffer (10 mM Tris–HCl, 10 mM ethylenediaminetetraacetic acid, 0.5 M NaCl; pH 8.0) containing 20 μg/ml RNase A (37 °C, 15 min), 2× SSC/0.1% NLS (37 °C, 20 min, twice), and 0.2× SSC/0.1% NLS (37 °C, 15 min, twice). Hybridization signals were visualized by alkaline phosphatase (AP) immunohistochemical staining using a DIG detection kit (Roche Diagnostics). Because ISH signals were so strong for *testican-2* and *SC1*, we shortened their reaction time (to 6–8 h) with nitro blue tetrazolium/5-Bromo-4-chloro-3-indolyl phosphate (NBT/BCIP) from the original reaction time (16–18 h) to prevent the saturation of ISH signals. Sections were mounted onto glass slides and dehydrated through a graded series of increasing ethanol concentration followed by xylene and then coverslipped with Entellan New (Merck, Tokyo, Japan).

Fluorescence double-labeling ISH was performed as described previously (Takahata et al. 2006). Fluorescein isothiocyanate (FITC)-labeled riboprobes for glutamic acid decarboxylase 67 (*GAD67*), vesicular glutamate transporter 1 (*VGluT1*), and glial fibrillary acidic protein (*GFAP*) were prepared. Brain sections were hybridized with both the DIG-labeled and the FITC-labeled probes. The hybridization protocol was the same as that of colorimetric single ISH. DIG was detected by staining with AP-conjugated anti-DIG antibodies and using an HNPP Fluorescence Detection kit (Roche Diagnostics). FITC was detected by horseradish peroxidase–conjugated anti-FITC antibodies (Roche Diagnostics) followed by enhancement using a TSA-Plus DNP system (Perkin Elmer Life Sciences, Boston, MA) and staining with Alexa 488–conjugated anti-DNP antibodies (Molecular Probes, Eugene, OR). The sections were then counterstained with Hoechst 30442 (Molecular Probes) diluted in PBS to 1:1000. After mounting onto glass slides, sections were air dried and coverslipped with the PermaFluor Aqueous mounting medium (Thermo, Pittsburgh, PA).

The brain regions of macaques were identified using brain atlases (Paxinos et al. 2000). Images of the ISH sections were captured with an SZX12 or BX50 microscope (Olympus, Tokyo, Japan) using a 3CCD color video camera, DP50 (Olympus), and processed using Photoshop CS3 Extended (Adobe, San Jose, CA). The scale bars in the figures are corrected for shrinkage caused by ISH.

IHC

Free-floating sections were immersed into the blocking buffer (2% bovine serum albumin [BSA], 0.5% Triton X-100 in tris-buffered saline [TBS] for Testican-1 IHC; 10% normal goat serum, 2% BSA, 0.5% Triton X-100 in TBS for SPARC IHC) for 1 h at room temperature. The sections were then reacted with the primary antibodies, goat anti-Testican-1-antiserum AF2327 (R&D systems, Minneapolis, MN, 2 μg/ml IgG), or mouse anti-SPARC-monoclonal antibody PP16 (Santa Cruz Biotechnology, Santa Cruz, CA, 1 μg/ml IgG) in the same blocking buffer overnight at 4 °C. The sections were then washed in TBS 3 times and reacted with the secondary antibodies conjugated with biotin for 2 h at room temperature. Finally, immunoreactivity was detected using an avidin/biotin/peroxidase detection kit (Vectastain, CA) and diaminobenzinine as a substrate, with nickel enhancement. The sections were dehydrated through a graded series of increasing ethanol concentrations followed by xylene and coverslipped with Entellan New. Sections developed without the primary antibodies showed no detectable signal above the background level (data not shown).

Quantification

The number of cells those contain fluorescent signal in double-labeling ISH was manually counted in V1 and TE. The images taken in 3 channels (ISH signals in red [*occ1*-related genes]/green [cell-type markers] channels and Hoechst nuclear staining in the blue channel) were layered into a single file. First, cortical layer boundaries were determined in reference to Hoechst nuclear staining. Then, the cells positive for green ISH fluorescent signal were plotted and counted in each cortical layer. Those cells that contain signals intense enough to be distinguished from background level were counted as positive cells. Finally, those cells that have the identical shape of red and green ISH fluorescent signals were counted as double-positive cells. Using the Hoechst nuclear staining, we confirmed that each of them has a single nucleus and the red and green signals are not derived from side by cells. Cells that had unclear ISH fluorescent signal due to the crowdedness of cells were excluded from the analysis.

To quantify the effect of MD on gene expression, the relative optical densities (RODs) of ISH signals in the bright field microscope were determined for the deprived or nondeprived ocular dominance column. We mainly used tangential/semitangential sections or coronal sections that showed wide ocular dominance columns for the analysis, in order to identify regions of each ocular dominance column. The shapes of each ocular dominance column were delineated with reference to the *occ1* ISH staining pattern in V1 tangential or coronal sections from 4 MD monkeys and applied to adjacent ISH sections for the other genes (see Fig. 10). The gray level of ISH signal for each gene and each column was converted into ROD using the following equation, $\mathrm{ROD} = \log_{10}(255/\text{observed gray levels})$.

The background ROD was subtracted from each ROD. The value of each ROD was then expressed as mean ± standard error of the mean, and the difference between deprived and nondeprived columns was determined by paired Student's *t*-test ($P < 0.05$ was considered significant).

Results

Identification of testican-1 as a V1-Enriched Gene by RLCS

To systematically identify area-specific molecules in the monkey neocortex, we carried out large-scale screening by RLCS. In this analysis, mRNAs were purified from 4 distinct cortical areas V1, TE, M1, and area 46, converted to cDNA by reverse transcription, and digested with a pair of restriction enzymes for 2D analysis. In ApaLI and HinfI enzyme combination, approximately 850 spots were obtained, and we found 86 apparent differential spots among the 4 cortical areas. Among them, one spot was particularly intense in the visual area (Fig. 1*A*). This spot was cloned and identified as the *testican-1* gene, a member of the gene family to which *occ1* belongs (Fig. 1*B*).

Expression Patterns of occ1-Related Genes in Macaque Neocortex

The identification of *testican-1* as a V1-enriched gene prompted us to carry out the comparative expression analysis of all the family genes of *occ1* in the monkey neocortex. Besides *occ1* and *testican-1*, there are 4 genes reported to belong to this family, namely, *testican-2*, *testican-3*, *SPARC*, and

SC1 (Vannahme et al. 1999; Nakada et al. 2001) (Fig. 1*B*). To estimate the differences in expression levels of those genes among different cortical areas, we carried out quantitative real-time RT-PCR using specific primers for *occ1*-related genes on cDNAs prepared from cortical samples of V1, TE, M1, S1, and area 46. We confirmed that *occ1* mRNA is particularly abundant in V1, compared with other areas (Fig. 1*C*), with *occ1* mRNA in V1 being about 3 times as abundant as that in M1 and association areas (TE and area 46). The expression level of *occ1* mRNA in S1 was approximately 1.5 times higher than those in M1 and association areas. The *testican-1* mRNA was also most abundant in V1, and its level was 2 times higher than that in association areas, validating the result of the RLCS analysis. Similarly, we observed that *testican-2* mRNA was also most abundant in V1, and its level was 1.2–1.4 times higher than that in other areas. No clear area difference was observed for *testican-3*, *SPARC*, and *SC1* in this analysis.

We further examined their mRNA expression in detail using ISH histochemistry. Figure 2 shows their expression patterns in 4 coronal sections of the macaque neocortex in low-magnification photographs. Consistent with the RT-PCR analysis results, we confirmed that both the *occ1* and *testican-1* ISHs exhibited a V1-enriched pattern. Similarly, *testican-2* mRNA signals were also observed to be abundant in V1, although the area difference was less conspicuous than those of *occ1* and *testican-1*. Both in S1 and A1, the mRNA signals of *occ1*, *testican-1*, and *testican-2* were also relatively strong. The mRNA signals of *testican-1* and *testican-2* were moderate in the higher association areas compared with those in V1 and other primary sensory areas. To our surprise, the staining pattern of ISH for *SPARC* showed clear area difference. Complementary to those of *occ1*, *testican-1*, and *testican-2*, the mRNA signals of *SPARC* were weak in V1 and strong in the higher association areas. The *SPARC* mRNA signals were also scarce in S1 and A1. Both *testican-3* and *SC1* ISH exhibited moderate or strong signals in the macaque neocortex, respectively, but the area differences in their expression were not observed.

Figure 3 shows magnified views of ISH sections for the *occ1* family genes in V1 and extrastriate visual cortices. As reported previously (Tochitani et al. 2001; Takahata et al. 2006), layer IVCβ was most strongly labeled by the *occ1* probe among the layers in V1. Strong signals were also observed in layers II/III of V1. Due to the strong V1 expression of *occ1* mRNA, the V1/V2 boundary was distinct (arrow in Fig. 3*A*). In extrastriate cortices, the *occ1* mRNA signals were localized mainly in pyramidal neurons that were present in the deeper part of layer III, and the signal intensity reduced along the visual ventral pathway (asterisks in Fig. 3*A–D*). Only faint *occ1* mRNA signals were observed in TE. The expression patterns of *testican-1* and *testican-2* mRNAs were quite similar to each other, and their area preferences were similar to that of *occ1*; that is, the *testican-1* and *testican-2* mRNA signals were strongest and densest in layer IVC of V1 (Fig. 3*E*,*I*), and thus, the V1/V2 boundary was clearly observed in their ISH. Pyramidal neurons in the deeper part of layer III were strongly labeled by the *testican-1* and *testican-2* probes in V2, and the signal intensity gradually decreased along the visual ventral pathway (Fig. 3*E–L*). Compared with those of *occ1*, the *testican-1* and *testican-2* mRNA signals in the visual cortices were stronger and more broadly distributed to other layers. Layer VIa also showed strong *testican-1* and *testican-2* mRNA signals and layers II, upper III, IV, and V of extrastriate cortices exhibited moderate *testican-1* and *testican-2* mRNA signals as well. The difference in the expression pattern between *testican-1* and *testican-2* was that the laminar specificity and area preference of the *testican-1* mRNA signal distribution were clearer than those of *testican-2* (Fig. 3*E–L*). The *testican-3* mRNA signals were sparsely distributed all across the visual cortices without apparent difference among layers and areas, except for layer I, which showed a low level of *testican-3* mRNA signal. The granule layer (layer IV) showed slightly strong *testican-3* mRNA signals (Fig. 3*M–P*). *SPARC*-mRNA-positive cells were observed on the surface of layer II and deeper layer VI (VIb) in V1, and little signal was observed in the other layers (Fig. 3*Q*). The *SPARC* ISH pattern in V2 was similar to that in V1, and thus, the V1/V2 boundary was not apparent in the ISH section for *SPARC*. The only difference in the *SPARC* mRNA expression between V1 and V2 was that the width of the *SPARC* mRNA

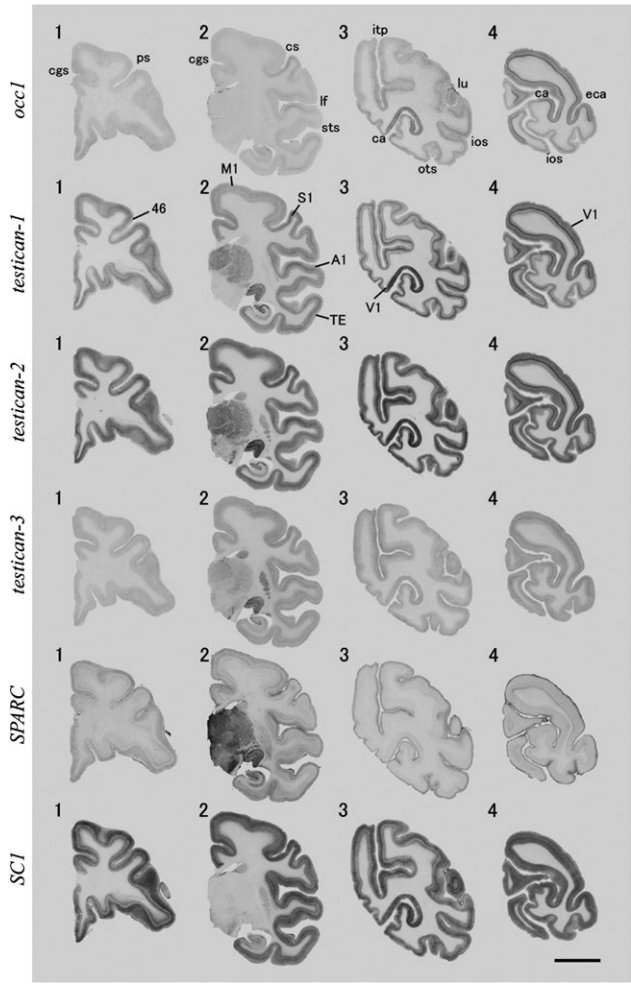

Figure 2. Expression patterns of *occ1*-related genes in coronal sections of adult monkey neocortex. For *occ1*, *testican-1*, and *testican-2*, note that the strongest signals were observed in V1, and moderate signals were observed in S1 and A1 as well (see the annotation in sections for *testican-1* ISH). Conversely, the expression of *SPARC* mRNA was strong in higher-order association areas, such as in TE, whereas weak in V1, S1, and A1. These sections corresponded to Bregma levels 8.5 (section 1), −14.4 (section 2), −32.8 (section 3), and −45.5 mm (section 4). ca/calcarine sulcus, cgs/cingulate sulcus, cs/central sulcus, eca/external calcarine sulcus, ios/inferior occipital sulcus, itp/intraparietal sulcus, lf/lateral fissure, lu/lunate sulcus, ots/occipitotemporal sulcus, and sts/superior temporal sulcus; scale bar = 10 mm.

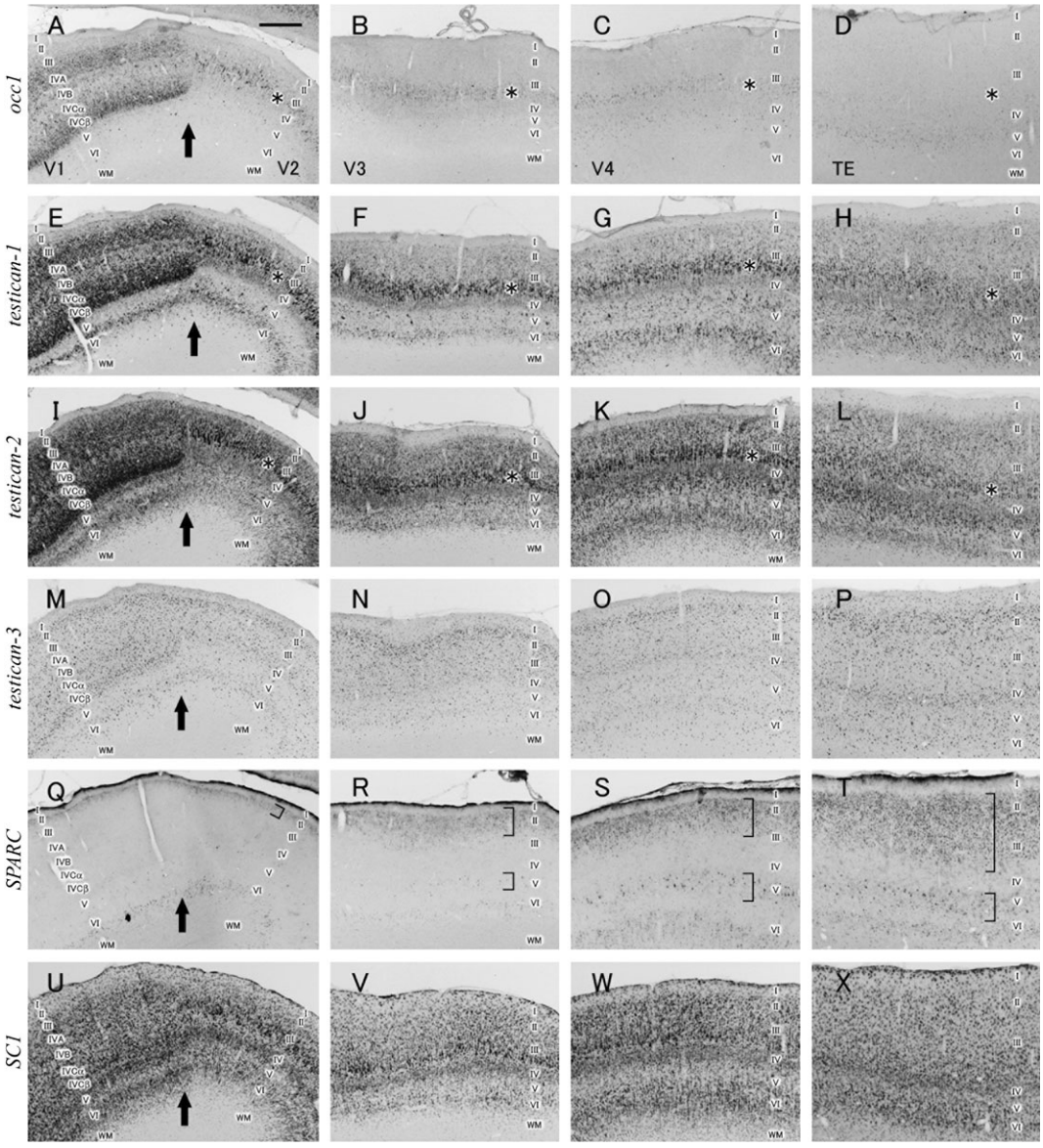

Figure 3. Higher magnification of coronal ISH sections for *occ1*-related genes in the visual cortices. The mRNA signals of *occ1*, *testican-1*, and *testican-2* were strongest in V1. Their signals in deeper layer III of the extrastriate cortices gradually decreased along the visual pathway (asterisks). Conversely, the *SPARC* mRNA expression was weak in V1 and gradually broadened in superficial layers and layer V along the visual pathway (brackets). WM/white matter; scale bar = 1.0 mm.

signals in layer II was slightly broadened into deeper layers in V2 compared with that in V1. Along the visual ventral pathway, the width of the *SPARC* mRNA signals in the supragranular layers further extended into deeper layers, and it almost covered the entire layers II/III in TE (brackets in Fig. 3*Q–T*). The *SPARC* mRNA signals also gradually increased along the pathway in layer V of extrastriate visual cortices. This expression pattern of the *SPARC* mRNA is very reminiscent of that of *retinal-binding protein (Rbp)*, which we have identified as an association area–enriched gene in the adult monkey neocortex (Komatsu et al. 2005). The abundance of the *SPARC* mRNA signals in layer VIb was not apparently different throughout the visual cortices. In addition, the *SPARC* mRNA signals were most strongly observed on the pial surface throughout the visual cortices, where neuronal cells are not present. The *SC1* mRNA signals were very strong throughout the neocortex and layers, including layer I (Fig. 3*U–X*). The *SC1* mRNA signals were more intense in layers IVC and VI of V1 than the other layers in V1, and signals in layers III, IV, and VI of extrastriate visual cortices were also strong.

We have already reported that the patchy distribution of the *occ1* mRNA signals in layers II/III of V1 coincides with CO-dense puffs or blobs (Takahata et al. 2006). We examined in V1 tangential sections whether other genes of this family were also enriched in blobs. We found that both the *testican-1* and *testican-2* mRNA signals were broadly distributed in tangential sections of layers II/III, but their expression levels were slightly higher in CO-rich blobs than in the remaining (interblob) regions (Fig. 4*A–D*). Notably, the distribution of the *SC1* mRNA signals exhibited clear enrichment in the CO-dense blobs (Fig. 4*E,F*). The *testican-3* and *SPARC* mRNA signals showed no such correlation with blobs (data not shown).

As ISH for *occ1*-related genes showed characteristic expression patterns in the visual circuit, we also examined their ISH in

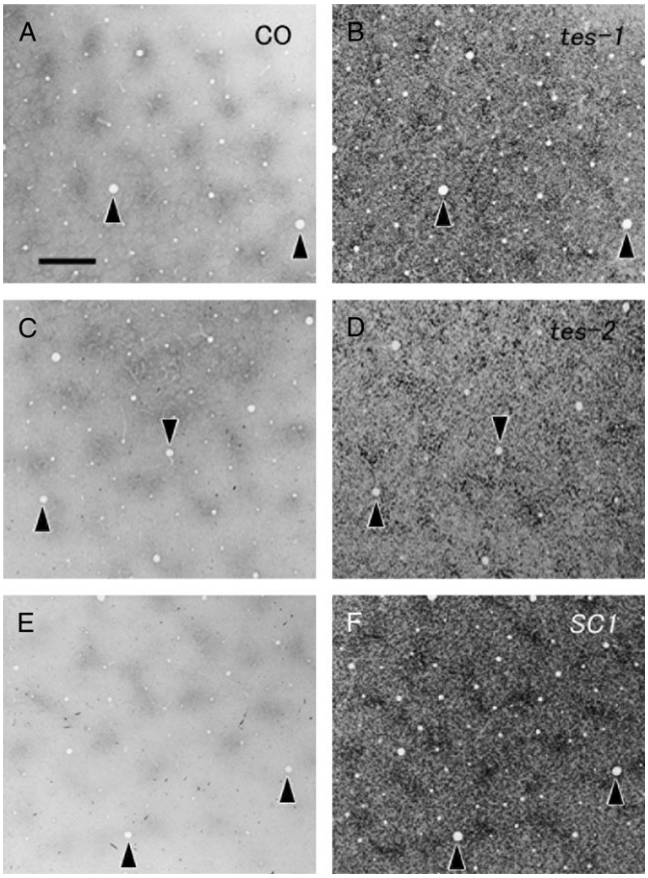

Figure 4. Tangential sections of ISH for *testican-1* (*B*), *testican-2* (*D*), and *SC1* (*F*) and adjacent sections reacted for CO enzymatic activity (*A*, *C*, *E*) in layers II/III of V1. Note that their expression patterns, particularly that of *SC1*, coincide with the CO-dense blobs of each respective panel on the left. Arrowheads indicate the same blood vessels. Scale bar = 500 μm.

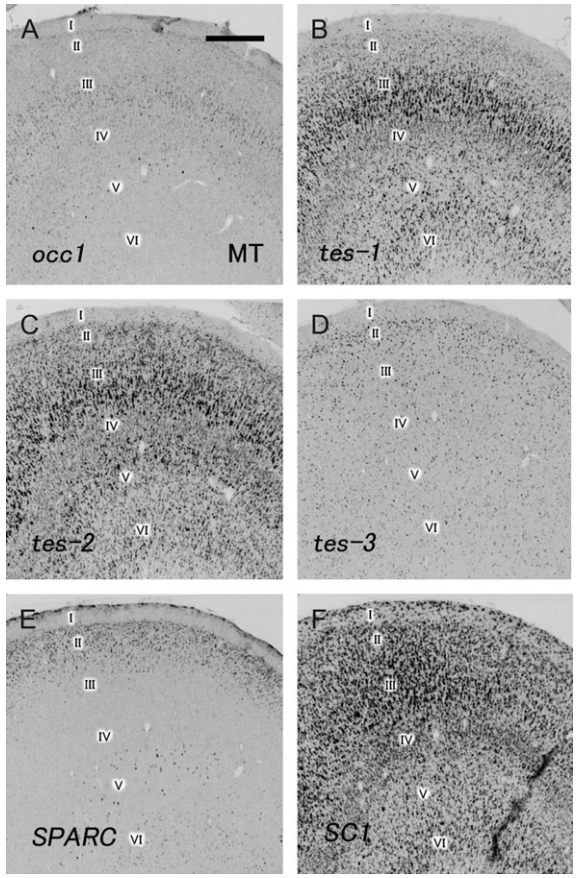

Figure 5. Expression patterns of *occ1*-related genes in coronal sections of MT. Their expression patterns were similar to those of the extrastriate cortex. Scale bar = 500 μm.

a distinct area of the primate visual system, the middle temporal visual area (MT), which is a highly myelinated compartment and the center of motion processing in the visual dorsal pathway (Kaskan and Kaas 2007). However, the expression patterns of *occ1*-related genes in MT were similar to those in extrastriate visual cortex and did not show clear demarcation with surrounding areas (Fig. 5).

Cell-Type Specificity in Expression of occ1-Related Genes in Visual Cortex

To identify the type of the cells that express *occ1*-related genes in the macaque neocortex, we carried out fluorescence double-labeling ISH with an excitatory neuron marker, *VGluT1*, and a GABAergic neuron marker, *GAD67*, as we had done to analyze *occ1*-mRNA-positive neurons in the previous study (Takahata et al. 2006). Furthermore, we used in this study an astrocyte marker, *GFAP*, because SPARC and SC1 proteins are reported to localize in glial cells in the brain (Johnston et al. 1990; Mendis et al. 1995; Mendis, Ivy, and Brown 1996). Below we first describe the double-labeling ISH experiments on *occ1*-related genes in V1. The *testican-1* mRNA signals colocalized with *VGluT1* (Fig. 6*A*) and *GAD67* mRNA signals (Fig. 6*B*) but not with the *GFAP* mRNA signals (Fig. 6*C*). This suggests that *testican-1* mRNA is expressed in both excitatory neurons and GABAergic interneurons but not in astrocytes in V1. Similarly, the *testican-2* mRNA signals colocalized with both *VGluT1* and *GAD67* mRNA signals but not with the *GFAP* mRNA signals in V1 (data not shown). In contrast to those of *testican-1* and *testican-2*, the *testican-3* mRNA signals predominantly colocalized with the *GAD67* mRNA signals, and colocalization with the *VGluT1* mRNA signals was rare, although low levels of *testican-3* mRNA signals colocalized with the *VGluT1* mRNA signals in layer IV (Fig. 6*D,E*). Colocalization of the *testican-3* mRNA signals with the *GFAP* mRNA signals was not observed (Fig. 6*F*). The *SPARC* mRNA signals in layer VIb predominantly colocalized with the *VGluT1* mRNA signals (Fig. 7*A*). The strong *SPARC* mRNA signals on the pial surface corresponded to the *GFAP* mRNA signals (Fig. 7*C*). Given that there were few *SPARC*-mRNA-positive cells, little colocalization of the *SPARC* mRNA signals with any markers was observed in the remaining layers of V1 (Fig. 7*A–C*). The *SC1* mRNA signals colocalized with both the *VGluT1* and *GAD67* mRNA signals in the granular and infragranular layers of V1 (Fig. 7*D,E*). The *SC1* mRNA signals also colocalized with the *GFAP* mRNA signals in superficial layers (Fig. 7*F*), although they appeared a different population from the *SPARC–GFAP*-double-positive cells.

In higher visual cortices, the cell-type specificity of *testican-1* (Fig. 8*A–C*), *testican-2*, *testican-3*, and *SC1* (data not shown)

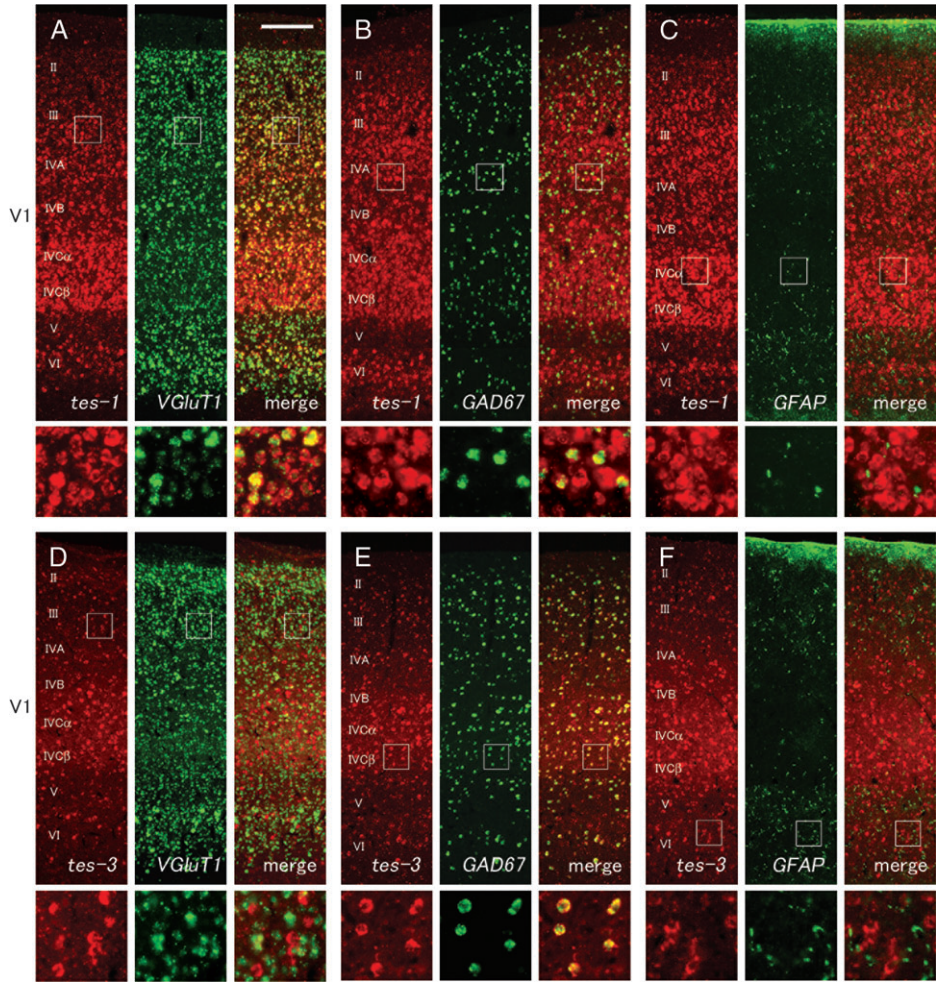

Figure 6. Coronal sections for double-labeling fluorescence ISH for *occ1*-related genes (red) and cell-type marker genes (green) in V1. (*A–C*) The *testican-1* mRNA signals colocalized well with both *VGluT1* (*A*) and *GAD67* (*B*) mRNA signals but not with *GFAP* mRNA signals (*C*). (*D–F*) The *testican-3* mRNA signals more predominantly colocalized with *GAD67* mRNA signals (*E*) than with *VGluT1* mRNA signals (*D*). They did not colocalize with *GFAP* mRNA signals (*F*). Small squares indicate the region where higher magnification photos, which are shown under each panel, were taken. Scale bar = 200 μm.

mRNA expression was essentially the same as that in V1, with the exception of *SPARC*. *SPARC* mRNA signals were rarely observed in layers II–V of V1; however, there were high levels of *SPARC* mRNA signals in layers II/III and V of TE. They colocalized well with both the *VGluT1* and *GAD67* mRNA signals (Fig. 8*D,E*). This indicated that *SPARC* mRNA expressions in excitatory and GABAergic neurons are similar for a particular cortical area. The *SPARC* mRNA signals on the pial surface in TE colocalized with the *GFAP* mRNA signals and those in layer IVb colocalized with the *VGluT1* mRNA signals (Fig. 8*D,F*) as well as in V1.

To calculate the proportion of either *testican-1*- or *SPARC*-mRNA-positive neurons to excitatory or GABAergic neurons of V1 and TE, we counted the number of cells positive for each mRNA (Table 1). The proportions of *testican-1*-mRNA-positive cells to *VGluT1*-mRNA-positive cells were high in layers of V1 and TE (>75%), except for infragranular layers of V1 (41.8%), where the expression is low in layers V and VIb. The proportions of *testican-1*-mRNA-positive cells to *GAD67*-mRNA-positive cells were approximately half (42.9–69.2%) in each layer of V1 and TE. On the other hand, the proportions of *SPARC*-mRNA-positive cells to *VGluT1*-mRNA-positive cells were very low in each layer of V1 (<15%), whereas those were remarkably higher in TE, especially in supragranular layers (3.6% in V1 and 71.0% in TE), which is consistent with our observation described above. The proportions of *SPARC*-mRNA-positive cells to *GAD67*-mRNA-positive cells were also higher in TE (19.8–38.5%) than in V1 (1.1–24.1%) throughout all the layers.

Immunohistochemical Identification of OCC1-Related Proteins

We examined IHC using anti-Testican-1 and anti-SPARC antibodies to reveal their protein localizations. In Testican-1 IHC, a consistently similar pattern to the ISH pattern was observed (Fig. 9*A–F*). There were abundant Testican-1 signals in layers II–IVA, IVC, and VI of V1 (Fig. 9*A,F*). IHC signals were also abundantly observed in layers deeper III, IV, and VI of extrastriate visual cortices and consistent with ISH data, Testican-1 protein signals in the thalamorecipient layers progressively decreased along the occipitotemporal visual pathway (Fig. 9*A,B*). At higher magnification, Testican-1 protein signals were detected in the neuronal cell bodies and proximal dendrites (Fig. 9*C–F*). It may be noted that a secreted form of

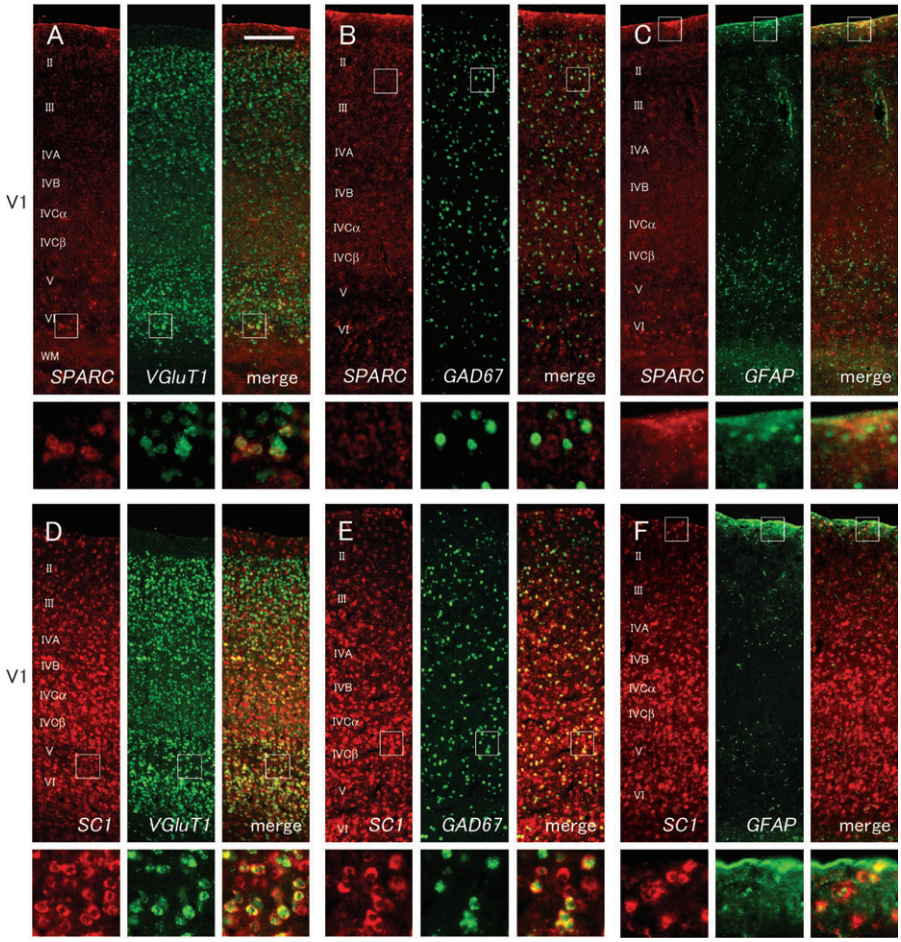

Figure 7. Continuation of Figure 6. (*A–C*) As *SPARC* mRNA signals were scarce in V1, they rarely colocalized with *VGluT1* (*A*) and *GAD67* (*B*) mRNA signals, except for the deepest layer (VIb), where colocalization between *SPARC* and *VGluT1* mRNA signals was observed. *SPARC* mRNA signals colocalized well with *GFAP* mRNA signals on the pial surface (*C*). (*D–F*) *SC1* mRNA signals colocalized well with both *VGluT1* and *GAD67* mRNA signals. They also colocalized with *GFAP* mRNA signals in superficial layers. Scale bar = 200 μm.

Testican-1 protein, if it exists, may be difficult to detect using IHC. In SPARC IHC, intense signals were detected only in the pial surface in all the cortical areas that were examined, which most likely corresponded to *SPARC* mRNA signals detected in astrocytes of the pial surface. At higher magnification, IHC signals were observed in glia-like small cells in the pial surface, and processes that are considered to be derived from astrocytes (Fig. 9*G–J*).

Activity Dependence in Expression of occ1-Related Genes in V1

We observed strong expression of *testican-1* and *testican-2* mRNAs in layer IVC and in blobs of V1 and in the deeper layer III of the extrastriate cortex. *SC1* mRNA expression was also strong in blobs. These observations raised the possibility that the transcriptions of those genes are driven by neuronal activity because those regions show more activity, as revealed by CO enzymatic reactivity, than others (Horton and Hubel 1981; Wong-Riley et al. 1989). Thus, we examined whether the expression of *occ1*-related genes, as with *occ1*, is dependent on sensory activity in V1 (Tochitani et al. 2001). ISH for *occ1* revealed periodical light and dark columns in the coronal sections of V1 in macaques of 5–21 days MD (Fig. 10*A*). In the adjacent coronal sections of ISH for *testican-1*, *testican-2*, and *SC1*, there was a partial decrease of the signal intensities in apparent deprived ocular dominance columns (Fig. 10*B–D*). To confirm that this reduction occurred in the deprived column, we examined ISH in the tangential sections of V1 in MD macaques. In both layers II/III and IVC, the decrease in the *occ1* mRNA expression was clearly observed, and the characteristic pattern of ocular dominance column staining was observed (Fig. 10*E,I*). In the ISH for *testican-1*, *testican-2*, and *SC1* in adjacent tangential sections of around layer IVC, the same pattern of ocular dominance column staining to that of *occ1* ISH was observed, presumably because of a significant decrease in their signals in the deprived columns (Fig. 10*J–L*), whereas such patterns were not observed in around layer III (Fig. 10*F–H*). To quantify the effects of MD on their expression, we measured their RODs in deprived and nondeprived columns and compared them between the 2 (Fig. 10*M–P*). The *occ1* mRNA expression showed a large and significant decrease in the ROD of the deprived columns both in layers III and IVC (23.5 ± 5.2%, $P < 0.05$ and 48.0 ± 2.9%, $P < 0.005$, respectively; $n = 4$ each). The *testican-1* and *testican-2* mRNA expressions also exhibited large and significant decreases in RODs owing to MD in layer IVC (16.4 ± 1.7%, $P < 0.05$ and 20.3 ± 1.7%, $P < 0.05$, respectively; $n = 4$ each). The reduction in the *SC1*

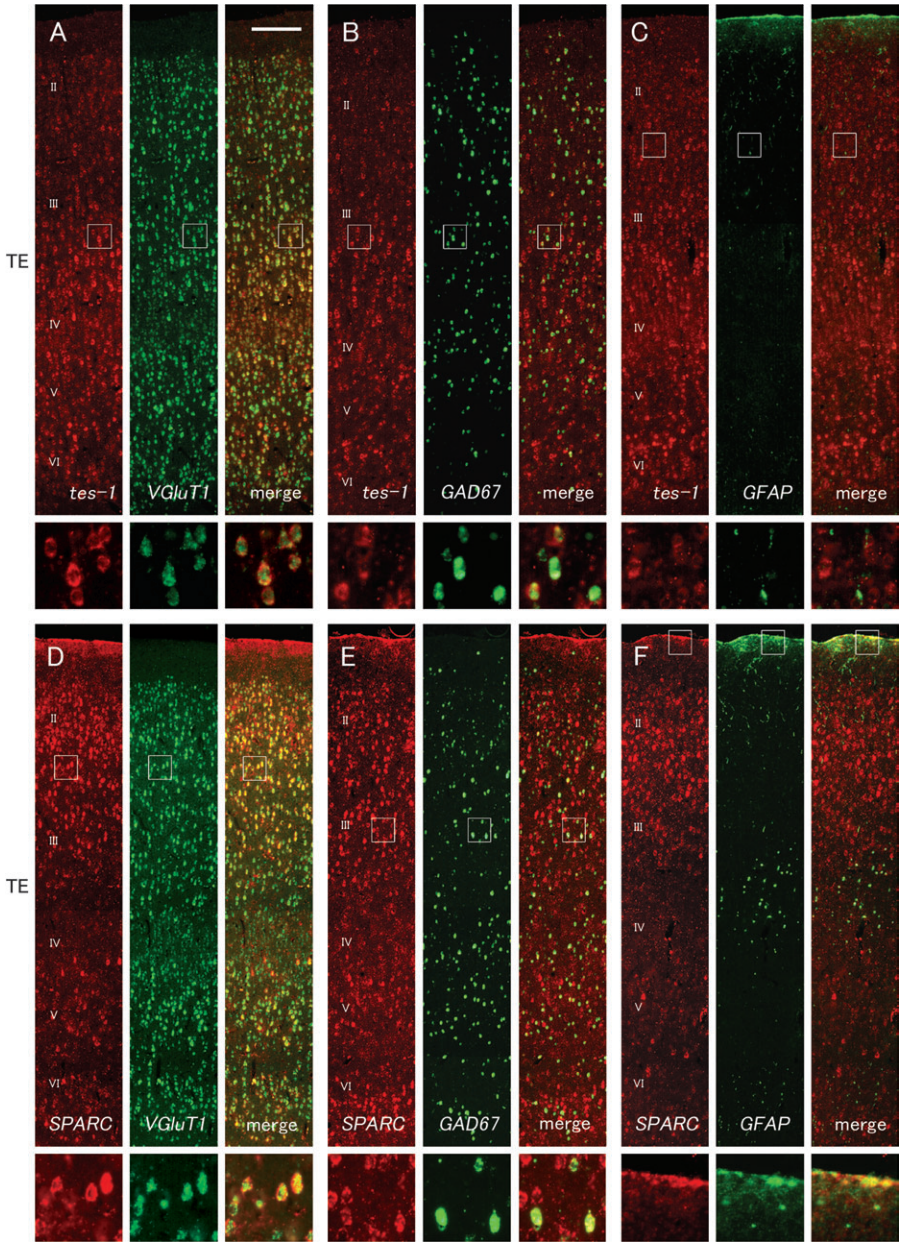

Figure 8. Coronal sections for double-labeling fluorescence ISH for *occ1*-related genes (red) and cell-type marker genes (green) in TE. (*A–C*) *testican-1* mRNA signals colocalized well with both *VGluT1* (*A*) and *GAD67* (*B*) mRNA signals but not with *GFAP* mRNA signals (*C*). (*D–F*) *SPARC* mRNA signals also colocalized with both *VGluT1* (*D*) and *GAD67* (*E*) mRNA signals. *SPARC* mRNA signals colocalized well with *GFAP* mRNA signals on the pial surface (*F*) as well as in V1. Scale bar = 200 μm.

mRNA signals was small (5.7 ± 1.3%) but statistically significant ($P < 0.05$; $n = 4$) in layer IVC. Significant reduction in mRNA expression of *testican-1*, *testican-2*, and *SC1* was not observed in layer III (4.2 ± 3.1%, $P = 0.41$, 5.7 ± 2.9%, $P = 0.15$ and 2.0 ± 1.9%, $P = 0.48$, respectively; $n = 4$ each). The effects of MD in the mRNA expression of *testican-3* and *SPARC* were not detected (data not shown).

Discussion

In this study, we examined the expression of *occ1*-related genes in cortical areas, particularly in the visual areas of macaque monkeys. We found that the area and laminar preferences of the *testican-1* and *testican-2* mRNA expressions were similar to that of *occ1*, whereas that of *SPARC* mRNA was complementary to them. Neurons in the blob regions exhibited high levels of *testican-1*, *testican-2*, and *SC1* mRNA expressions. These suggested that their expressions are linked to neuronal connectivity. The activity-dependent regulation of *testican-1*, *testican-2*, and *SC1* mRNA expression in V1 also raised the possibility of a functional involvement in synaptic plasticity. In earlier studies, we reported unique area- and lamina-associated expression of *occ1* and *Rbp* and their complementary patterns in the monkey neocortex (Yamamori and Rockland 2006). The novelty of the present study is the finding that a particular paralogous group of genes exhibit similar or complementary expressions, in relation to the anatomical architecture of the sensory and association cortex

in an orderly manner, and that this closely resembles the laminar and area specificity of *occ1* and *Rbp*.

Anatomical Architecture and Molecular Distribution

The *occ1*, *testican-1*, and *testican-2* genes are abundantly expressed in layer IVC of V1, blobs and deeper layer III of the extrastriate visual cortex, and scarce in higher-order areas. This graded distribution pattern resembles the immunoreactivities of PV, which reveal the distribution of thalamocortical projection fibers (Hashikawa et al. 1995; Levitt et al. 1995; Rockland et al. 1999). The same kind of graduation is also exhibited by CO enzymatic activity (Wong-Riley 1994). On the other hand, the expression of *SPARC*, as well as *Rbp*, seems to avoid the thalamorecipient layers, and thus, this expression pattern also resembles the graded distribution of zinc-enriched terminations, which represent a subset of nonthalamocortical glutamatergic synapses (Ichinohe and Rockland 2005). Similar increasing chemical gradients of GluR2/3 and calbindin D-28K outside the granular layer along the visual pathway have also been reported (Kondo et al. 1994; Xu et al. 2003).

Table 1
The estimation of percentage of *testican-1*- or *SPARC*-mRNA-positive cells to *VGluT1*- or *GAD67*-mRNA-positive cells in V1 and TE

	V1		TE	
testican-1	Layer	Double/*VGluT1*	Layer	Double/*VGluT1*
	II/III	75.4% (1284/1743)	II/III	78.2% (1855/2396)
	IVC	96.0% (1084/1139)	IV	88.5% (724/824)
	V/VI	41.8% (846/2431)	V/VI	87.5% (1349/1568)
	Layer	Double/*GAD67*	Layer	Double/*GAD67*
	II/III	42.9% (323/972)	II/III	69.2% (768/1151)
	IVC	64.4% (338/556)	IV	55.9% (157/295)
	V/VI	52.3% (239/491)	V/VI	55.0% (183/347)
SPARC	Layer	Double/*VGluT1*	Layer	Double/*VGluT1*
	II/III	3.6% (49/1479)	II/III	71.0% (1567/2209)
	IVC	0.3% (3/1003)	IV	16.0% (148/936)
	V/VI	13.0% (187/1488)	V/VI	48.3% (792/1707)
	Layer	Double/*GAD67*	Layer	Double/*GAD67*
	II/III	24.1% (164/680)	II/III	38.5% (414/1098)
	IVC	1.1% (6/530)	IV	19.8% (49/258)
	V/VI	5.5% (17/310)	V/VI	22.2% (91/409)

Note: Figures in the brackets indicate numbers of counted cells those are double positive for *testican-1* or *SPARC* and cell-type marker (*VGluT1* or *GAD67*) out of numbers of counted cells those are positive for particular cell-type marker (*VGluT1* or *GAD67*).

Overall, there seems to be 2 opposing patterns of neurochemical gradient between V1 and TE, which are represented by the *occ1* and *Rbp* patterns. It has been reported that there are gradients in timing of maturation, dendritic field size of pyramidal neurons, and susceptibility of synaptic plasticity among occipitotemporal visual pathways (Murayama et al. 1997; Elston and Rosa 1998; Bourne and Rosa 2006). These features may be due to the molecules that exhibit gradual distribution along the visual pathway of the neocortex, by regulating cell maturation, arbor extension, and physiological properties.

Unlike the correspondence of *occ1* mRNA expression with blobs to which we described as activity-dependent regulation (Takahata et al. 2006), this is not the case for *SC1*. Interestingly, *SC1* mRNA was also selectively expressed in the koniocellular layers of the dorsal lateral geniculate nucleus (dLGN) (Takahata and Yamamori, unpublished data), which presumably send thalamocortical axons to blob regions (Ding and Casagrande 1998). The *occ1* mRNA is only weakly expressed in the magnocellular layers of dLGN (Tochitani et al. 2001), which mainly send axons to layer IVCα of V1 (Callaway 1998). Thus, the *SC1* mRNA expression may reflect a specific type of projections rather than neuronal activity.

Cell-Type Specificity in Expression of occ1-Related Genes

We have already demonstrated that the pronounced area-specific expressions of *occ1* and *Rbp* are primarily due to their

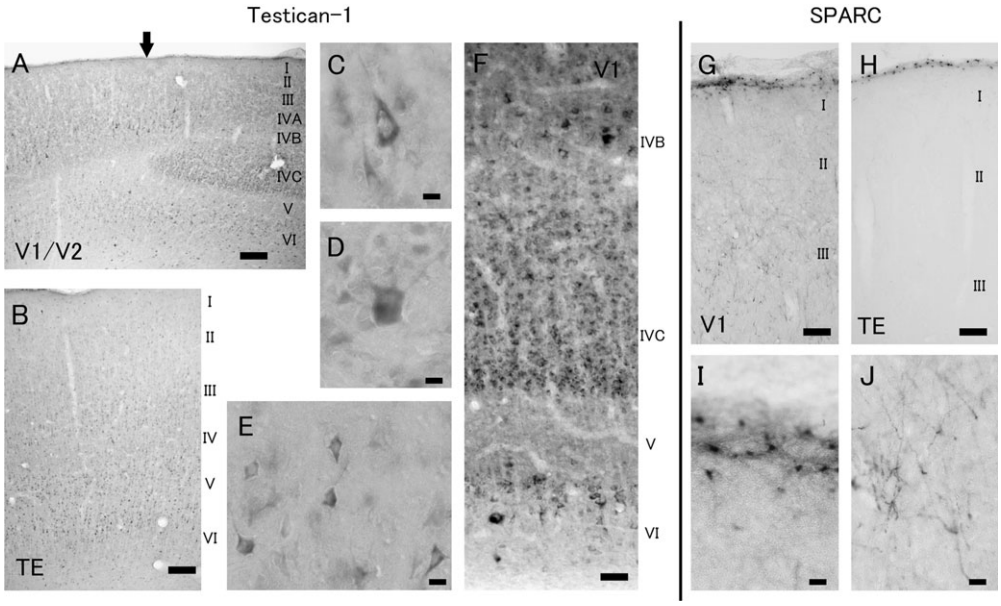

Figure 9. Immunohistochemical analysis of Testican-1 (*A–F*) and SPARC (*G–J*) expression in the monkey neocortex. (*A*, *B*) IHC for Testican-1 in V1 (*A*) and TE (*B*) showed patterns very similar to those obtained by ISH at a glance. The arrow in (*A*) shows the V1/V2 boundary. (*C–E*) High power images of Testican-1-positive neurons in layer III of V2 (*C*) and layer V of V2 (*D*) and TE (*E*). The immunoreactivity was mainly observed in the cell body and proximal neurite. (*F*) Immunostaining with anti-Testican-1-antiserum in V1. (*G*, *H*) IHC for SPARC in V1 (*G*) and TE (*H*). In this staining, SPARC signals were only observed in the astrocyte-like cells. (*I*, *J*) High power images of SPARC immunoreactivity in the pial surface (*I*) and layer III (*J*) of V1. Scale bar in (*A*, *B*) = 400 μm, scale bar in (*C–E*) = 10 μm, scale bar in (*F*) = 80 μm, scale bar in (*G*, *H*) = 80 μm, and scale bar in (*I*, *J*) = 10 μm.

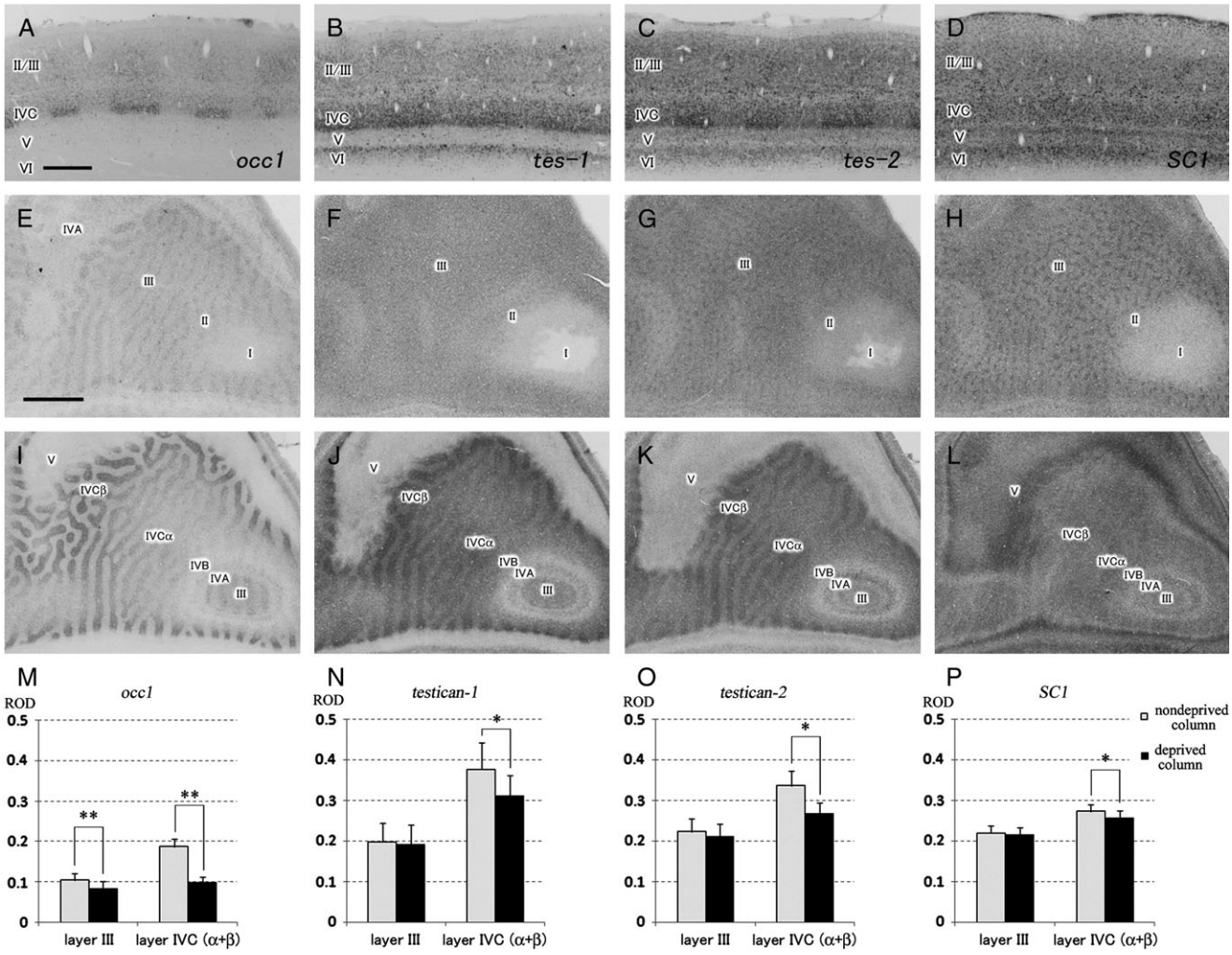

Figure 10. Coronal (*A–D*) and tangential (*E–L*) sections of ISH for *occ1*-related genes in the MD monkey V1. (*E–H*) are from layer III, and (*I–L*) are from layer IVC. The expressions of *occ1* (*A*, *I*), *testican-1* (*B*, *J*), *testican-2* (*C*, *K*), and *SC1* (*D*, *L*) mRNA were significantly downregulated in the deprived columns by MD in layer IVC. In layer III, whereas *occ1* mRNA expression was significantly downregulated (*E*), the expressions of *testican-1* (*F*), *testican-2* (*G*), and *SC1* (*H*) were not affected. (*M–P*) Measurement of RODs for each gene in deprived and nondeprived columns in layers III and IVC. $*/P < 0.05$; $**/P < 0.01$ ($n = 4$, each data); scale bar in (*A*) = 500 μm for (*A–D*), scale bar in (*E*) = 1.0 mm for (*E–L*).

expressions in excitatory neurons (Komatsu et al. 2005; Takahata et al. 2006). The pronounced expression of *occ1* is observed in excitatory neurons of thalamorecipient layers in V1, whereas the *occ1* expression in inhibitory neurons is observed throughout all the layers of the neocortical areas examined (Takahata et al. 2006). As we have shown above, *testican-3* mRNA, which does not show clear area difference or activity dependence, is expressed predominantly in GABAergic inhibitory interneurons. This difference supports our idea that the gene expression in excitatory neurons mainly comprises of area-selective and activity-related patterns.

The proportions of *testican-1* mRNA expression to either excitatory or GABAergic neurons were not evidently different between V1 and TE, which suggest that it is the difference in the level of expression per cell, rather than in the probability whether or not a cell is determined to express the gene, is a main factor in the area selectivity of *testican-1* mRNA expression. In this regard, it is unclear whether the area selectivity of *testican-1* and *testican-2* mRNA expressions is exclusively due to the expression in excitatory neurons. In case of *SPARC*, it is obvious that the expressions in excitatory and GABAergic neurons both contribute to the overall area selectivity of *SPARC* mRNA expression. This observation was unexpected because excitatory glutamatergic neurons and the majority of GABAergic interneurons are presumably different in their developmental origins (Kornack and Rakic 1995; Tan et al. 1998). Therefore, the expression pattern of *SPARC* mRNA may be established after the formation of cortical areas and the tangential migration of GABAergic interneurons. Alternatively, *SPARC*-mRNA–containing GABAergic neurons may have similar origin to excitatory neurons. In humans, it is reported that more than half of GABAergic neurons originate from progenitors in the neocortical ventricular and subventricular zones of the dorsal forebrain (Letinic et al. 2002). In either case, the establishment of area-selective gene expression might be initially regulated by several differential mechanisms and finally tuned in a coordinated manner.

Consistent with previous studies (Johnston et al. 1990; Mendis et al. 1995; Mendis, Ivy, and Brown 1996; Liu et al. 2005; Vincent et al. 2008), we found that *SPARC* and *SC1* mRNA expressions are observed not only in neurons but also in glial cells. We have demonstrated that their heterogeneous distributions in the

neocortex are only observed in the neurons and that no particular area preference in glial expression was found for these genes. Their expressions in glial cells would obscure the regional preference of neuronal expressions both in the real-time PCR and histochemistry. The *SPARC* or *SC1* mRNA expressions in neurons showed clearer structure-related boundaries than the overall appearance that includes those of glial cells.

IHC revealed that the protein localization of Testican-1 parallels that of *testican-1* transcripts. This observation evidently demonstrates the existence of the same type of heterogeneity in the macaque neocortex in the protein level as in the mRNA level. This is inconsistent with the report that the Testican-1 protein exclusively localizes in the postsynaptic region of neurons in the mouse cortex (Bonnet et al. 1996). Although the exact reason for this discrepancy is not known, one possible explanation is that posttranscriptional and/or posttranslational modifications of *testican-1* gene are different between mice and macaques. We also confirmed the reduction of immunoreactivity of Testican-1 after MD (data not shown). SPARC IHC only showed signals in the astrocytes and their processes in the pial surface and not in cortical neurons. This inconsistent observation of IHC signals with ISH signals is likely attributable to the differential detection sensitivity between the 2 methodologies, that is, the neuronal expression of SPARC is too weak to be detected in IHC (also note that *testican-1* ISH signals are much stronger than Testican-1 IHC signals). The strength of IHC signals can be weakened due to low specificity of antibody, inappropriate fixation, and diffusion of targeted protein. Nonetheless, it is possible that the neuronal translation of SPARC is indeed considerably weak or SPARC proteins are substantially secreted from neurons, and they are too diffusely localized to be sensitive to IHC.

Possible Function of OCC1-Related Proteins in Visual Processing and Plasticity

The OCC1-related proteins are all multifunctional secreted glycoproteins and considered to be components of the ECM (Yan and Sage 1999). They are classified on the basis of their FS and EC domain structures. In addition to these common motifs, each protein of the OCC1 family has their original domains in the *N*-terminal or both the *N*- and *C*-terminals (Fig. 1*B*) (Vannahme et al. 1999). Other than the genes described in this paper, the structures of SMOC-1 and SMOC-2 have a partial similarity with those of OCC1-related proteins (Vannahme et al. 2003). However, their expressions did not show any clear area preference (data not shown). It is reported that Testican-3 has an alternative splicing variant form, N-Tes, which lacks the C-terminal domain of Testican-3 (Nakada et al. 2001). The expression level of *N-tes* mRNA was too low to be detected by ISH and RT-PCR (data not shown).

Lines of evidence suggest that ECM proteins modulate neuronal development and plastic changes. Several groups have proposed that ECM limits plasticity in the rodent neocortex and ECM degeneration is required to implement ocular dominance plasticity (Pizzorusso et al. 2002; Oray et al. 2004). Secreted glycoproteins, such as Reelin, regulate both neuronal positioning in the developing nervous system and synaptic plasticity in the adult (Bock and Herz 2003; Dityatev and Schachner 2006).

Although it is not as plastic as in the nervous systems of juvenile animals, matured nervous systems also respond to sensory and motor experiences by reorganizing cortical circuitry (Sawtell et al. 2003; Giannikopoulos and Eysel 2006; O'Shea et al. 2007), and spines are dynamic even in matured neocortex (Majewska et al. 2006). In addition, there is evidence that the characteristics of plasticity are different among cortical areas. For example, it has been reported that the dendritic spine motility level is low in V1 among cortical areas in adult mice (Majewska et al. 2006). Discontinuous brief high-frequency electrical stimulation of the horizontal pathway in layers II/III pyramidal neurons induces long-term potentiation of extracellular field potentials in layers II/III of TE in adult macaques, whereas the same treatment conversely induces long-term depression in layers II/III of V1 (Murayama et al. 1997). Together with the area selectivity and activity dependence in expression of *occ1*-related genes, these observations raise a possibility that OCC1-related proteins modulate synaptic plasticity in the adult cerebral cortex.

As an intriguing hypothesis, the activity of matrix metalloproteinases (MMPs), which play crucial roles in neuronal plasticity through degradation of ECM and synapse apparatus in brains (Dzwonek et al. 2004; Monea et al. 2006), may be regulated in different ways among areas by OCC1-related proteins. OCC1-related proteins have a Kazal-like motif that is associated with serine protease inhibition in their FS domains (Alliel et al. 1993). More directly, the *N*-domains of Testican-1 and Testican-3 are shown to inhibit protease activity of MT1-MMP in cancer tissues (Nakada et al. 2001). Conversely, Tremble et al. (1993) suggested that SPARC induces MMP expression in fibroblasts. If OCC1-related proteins regulate the MMP activity in macaque neocortex, then they may play a role in stabilizing synapses through the suppression of MMPs in active neurons of V1 and allow plasticity to occur in higher-order areas. Once retinal activity is silenced, the expressions of *occ1*-related genes may be downregulated, allowing neuronal remodeling of visual areas where the silenced retina had projected. Additionally, the idea that OCC1-related proteins are involved in stabilization of ECM may also explain the fact that the dendritic field area of layer III pyramidal neurons, as well as their horizontal axon field size, progressively increases along the visual ventral pathway (Elston and Rosa 1998; Tanigawa et al. 2005) because ECM can limit the neurite extension and MMP can release it (Hayashita-Kinoh et al. 2001). Consistently, Testican-1 and Testican-2 have been shown to inhibit neurite outgrowth in cultured cells (Marr and Edgell 2003; Schnepp et al. 2005).

Glial expressions of SPARC and SC1 are well studied in rodents. Their expressions are similar to those in macaques as described here, suggesting that their function has been conserved through the course of evolution. Brown's group suggested the possibility that the pial SPARC regulates angiogenesis from the pia, interacting with platelet-derived growth factor, thrombospondin, basic fibroblast growth factor, and others (Mendis and Brown 1994). In addition, they have also hypothesized that SC1 is involved in synaptogenesis, based on its expression pattern and protein localization in post-synapse apparatus and perisynaptic glial processes, and its anticell adhesion ability (Lively et al. 2007; Lively and Brown 2008). Both SPARC and SC1 expressions in the brain are induced under stressful conditions such as seizure, brain injury, morphine intoxication, and axon deafferentation (Mendis et al. 1998, 2000; Ikemoto et al. 2000; Liu et al. 2005; Lively and Brown 2007), suggesting that they have protective roles against harmful assaults to the brain. This kind of glial expression

under gliosis has also been reported for human Testican-1 (Marr et al. 2000).

The significance of the differential expression among *occ1*-related genes is still unclear. As such, questions include: 1) Why are the expression patterns of *occ1*, *testican-1*, and *testican-2* genes alike in spite of their functional differences? That is, it has been suggested that Testican-2 interacts with other Testican family proteins (Nakada et al. 2003), and OCC1 has lost its ability to bind extracellular calcium in the course of molecular evolution (Hambrock et al. 2004). 2) Why is *testican-3* mRNA predominantly expressed in GABAergic interneurons? 3) Why is *SC1* mRNA expression in blobs not downregulated after MD? Modification of the basic functions may result in significantly heterogeneous extracellular environments among distinct cortical areas. Detailed functional assays are required to elucidate the roles of OCC1-related proteins in the cerebral cortex.

Significance of occ1-Related Genes in Brain Evolution

One of our primary motivations in the investigation of area-specific genes is what they can tell us about the evolution of the primate neocortex. We previously showed that the characteristic V1-enriched expression pattern of *occ1* is conserved between macaques and marmosets but is absent in mice, rabbits, and ferrets (Takahata et al. 2006). Moreover, the expression of the orthologue gene of *occ1*, *occ1/Frp*, in mouse sensory domains is not downregulated by sensory ablation (Takahata et al. 2008). Thus, we currently consider that the V1-selective and activity-dependent *occ1* mRNA expression was uniquely acquired by the primate lineage during the course of evolution.

The *testican-1* and *testican-2* mRNA expressions have been shown to be distributed strongly and evenly throughout the adult mouse neocortex (Bonnet et al. 1996; Vannahme et al. 1999). According to Mendis and Brown (1994; Mendis, Shahin, et al. 1996), the expression intensities of *SPARC* and *SC1*, at both the mRNA and protein levels, do not differ among cortical areas in mice, although the *SPARC* expression shows an anterior–posterior gradient in the entire brain. Consistent with these reports, there is no evidence for area-related differential expression of *occ1*-related genes in adult mice (either from the database [http://www.brain-map.org/welcome.do] or from our preliminary experiments). However, the results of RNA dot blot analysis in the human neocortex suggested that *testican-1* mRNA is most abundantly expressed in the occipital lobe and most scarcely expressed in the frontal lobe (Marr et al. 2000) (ca. 1.4 times richer in the occipital lobe than in the frontal lobe). Our preliminary experiment suggested that *testican-1* and *testican-2* mRNAs are preferentially expressed in V1 of both marmosets and squirrel monkeys (data not shown). These are consistent with our present data in macaques and in view of these findings, we consider that the area-selective expression patterns of *occ1*-related genes may also be present exclusively in the primate lineage.

All the members of the *occ1* family of genes are present in the genome of various vertebrates and their amino acid sequences are well conserved, suggesting an ancient origin and a functional importance of these genes. Nevertheless, their transcriptional regulatory systems in neuronal cells appear markedly altered in the cerebral cortex in the primate lineage. We suggest that this alteration is tightly and specifically correlated with the evolution of the architecture in primates. In this sense, further studies on *occ1*-related genes will provide molecular clues to understanding the basis of the anatomical heterogeneity of the primate cerebral cortex.

Supplementary Material

Supplementary Table 1 can be found at: http://www.cercor.oxfordjournals.org/.

Funding

A Grant-in-Aid for Scientific Research on Priority Areas (Molecular Brain Science) from the Ministry of Education, Culture, Sports, Science, and Technology of Japan to T.Y. Funding to pay the Open Access publication charges of this article was provided by a Grant-in-Aid for scientific research on priority areas (Molecular Brain Science) from the Ministry of Education, Culture, Sports, Science, and Technology of Japan (#17024055).

Notes

We thank Dr Takehiko Kobayashi, National Institute of Genetics, for his help in the real-time PCR experiment and Kaoru Sawada, NIBB, for her preparation of monkey cDNAs. We also thank Dr Kathleen S. Rockland, RIKEN, for her critical reading of this manuscript, Dr Hiroshi Sato, Kanazawa University, for his informative discussion about the function of Testican family genes, and Peiyan Wong, Vanderbilt University, for her proofreading of the manuscript. *Conflict of Interest*: None declared.

Address correspondence to Tetsuo Yamamori, Division of Brain Biology, National Institute for Basic Biology, 38 Nishigonaka, Myodaiji, Okazaki, Aichi 444-8585, Japan. Email: yamamori@nibb.ac.jp.

References

Alliel PM, Perin JP, Jolles P, Bonnet FJ. 1993. Testican, a multidomain testicular proteoglycan resembling modulators of cell social behaviour. Eur J Biochem. 214:347–350.

Bock HH, Herz J. 2003. Reelin activates SRC family tyrosine kinases in neurons. Curr Biol. 13:18–26.

Bonnet F, Perin JP, Charbonnier F, Camuzat A, Roussel G, Nussbaum JL, Alliel PM. 1996. Structure and cellular distribution of mouse brain testican. Association with the postsynaptic area of hippocampus pyramidal cells. J Biol Chem. 271:4373–4380.

Bourne JA, Rosa MG. 2006. Hierarchical development of the primate visual cortex, as revealed by neurofilament immunoreactivity: early maturation of the middle temporal area (MT). Cereb Cortex. 16:405–414.

Callaway EM. 1998. Local circuits in primary visual cortex of the macaque monkey. Annu Rev Neurosci. 21:47–74.

Ding Y, Casagrande VA. 1998. Synaptic and neurochemical characterization of parallel pathways to the cytochrome oxidase blobs of primate visual cortex. J Comp Neurol. 391:429–443.

Dityatev A, Schachner M. 2006. The extracellular matrix and synapses. Cell Tissue Res. 326:647–654.

Dzwonek J, Rylski M, Kaczmarek L. 2004. Matrix metalloproteinases and their endogenous inhibitors in neuronal physiology of the adult brain. FEBS Lett. 567:129–135.

Elston GN, Rosa MG. 1998. Morphological variation of layer III pyramidal neurones in the occipitotemporal pathway of the macaque monkey visual cortex. Cereb Cortex. 8:278–294.

Giannikopoulos DV, Eysel UT. 2006. Dynamics and specificity of cortical map reorganization after retinal lesions. Proc Natl Acad Sci USA. 103:10805–10810.

Hamasaki T, Leingartner A, Ringstedt T, O'Leary DD. 2004. EMX2 regulates sizes and positioning of the primary sensory and motor areas in neocortex by direct specification of cortical progenitors. Neuron. 43:359–372.

Hambrock HO, Kaufmann B, Muller S, Hanisch FG, Nose K, Paulsson M, Maurer P, Hartmann U. 2004. Structural characterization of TSC-36/Flik: analysis of two charge isoforms. J Biol Chem. 279: 11727–11735.

Hashikawa T, Molinari M, Rausell E, Jones EG. 1995. Patchy and laminar terminations of medial geniculate axons in monkey auditory cortex. J Comp Neurol. 362:195–208.

Hayashita-Kinoh H, Kinoh H, Okada A, Komori K, Itoh Y, Chiba T, Kajita M, Yana I, Seiki M. 2001. Membrane-type 5 matrix metalloproteinase is expressed in differentiated neurons and regulates axonal growth. Cell Growth Differ. 12:573–580.

Horton JC, Hubel DH. 1981. Regular patchy distribution of cytochrome oxidase staining in primary visual cortex of macaque monkey. Nature. 292:762–764.

Ichinohe N, Rockland KS. 2005. Zinc-enriched amygdala- and hippocampo-cortical connections to the inferotemporal cortices in macaque monkey. Neurosci Res. 53:57–68.

Ikemoto M, Takita M, Imamura T, Inoue K. 2000. Increased sensitivity to the stimulant effects of morphine conferred by anti-adhesive glycoprotein SPARC in amygdala. Nat Med. 6:910–915.

Job C, Tan SS. 2003. Constructing the mammalian neocortex: the role of intrinsic factors. Dev Biol. 257:221–232.

Johnston IG, Paladino T, Gurd JW, Brown IR. 1990. Molecular cloning of SC1: a putative brain extracellular matrix glycoprotein showing partial similarity to osteonectin/BM40/SPARC. Neuron. 4:165–176.

Kaskan PM, Kaas JH. 2007. Cortical connections of the middle temporal and the middle temporal crescent visual areas in prosimian galagos (Otolemur garnetti). Anat Rec (Hoboken). 290:349–366.

Komatsu Y, Watakabe A, Hashikawa T, Tochitani S, Yamamori T. 2005. Retinol-binding protein gene is highly expressed in higher-order association areas of the primate neocortex. Cereb Cortex. 15:96–108.

Kondo H, Hashikawa T, Tanaka K, Jones EG. 1994. Neurochemical gradient along the monkey occipito-temporal cortical pathway. Neuroreport. 5:613–616.

Kornack DR, Rakic P. 1995. Radial and horizontal deployment of clonally related cells in the primate neocortex: relationship to distinct mitotic lineages. Neuron. 15:311–321.

Lein ES, Hawrylycz MJ, Ao N, Ayres M, Bensinger A, Bernard A, Boe AF, Boguski MS, Brockway KS, Byrnes EJ, et al. 2007. Genome-wide atlas of gene expression in the adult mouse brain. Nature. 445:168–176.

Letinic K, Zoncu R, Rakic P. 2002. Origin of GABAergic neurons in the human neocortex. Nature. 417:645–649.

Levitt JB, Yoshioka T, Lund JS. 1995. Connections between the pulvinar complex and cytochrome oxidase-defined compartments in visual area V2 of macaque monkey. Exp Brain Res. 104:419–430.

Liu X, Ying G, Wang W, Dong J, Wang Y, Ni Z, Zhou C. 2005. Entorhinal deafferentation induces upregulation of SPARC in the mouse hippocampus. Brain Res Mol Brain Res. 141:58–65.

Lively S, Brown IR. 2007. Analysis of the extracellular matrix protein SC1 during reactive gliosis in the rat lithium-pilocarpine seizure model. Brain Res. 1163:1–9.

Lively S, Brown IR. 2008. Localization of the extracellular matrix protein SC1 coincides with synaptogenesis during rat postnatal development. Neurochem Res. 33:1692–1700.

Lively S, Ringuette MJ, Brown IR. 2007. Localization of the extracellular matrix protein SC1 to synapses in the adult rat brain. Neurochem Res. 32:65–71.

Majewska AK, Newton JR, Sur M. 2006. Remodeling of synaptic structure in sensory cortical areas in vivo. J Neurosci. 26:3021–3029.

Marr HS, Basalamah MA, Bouldin TW, Duncan AW, Edgell CJ. 2000. Distribution of testican expression in human brain. Cell Tissue Res. 302:139–144.

Marr HS, Edgell CJ. 2003. Testican-1 inhibits attachment of Neuro-2a cells. Matrix Biol. 22:259–266.

Maurer P, Hohenadl C, Hohenester E, Gohring W, Timpl R, Engel J. 1995. The C-terminal portion of BM-40 (SPARC/osteonectin) is an autonomously folding and crystallisable domain that binds calcium and collagen IV. J Mol Biol. 253:347–357.

Mendis DB, Brown IR. 1994. Expression of the gene encoding the extracellular matrix glycoprotein SPARC in the developing and adult mouse brain. Brain Res Mol Brain Res. 24:11–19.

Mendis DB, Ivy GO, Brown IR. 1996. SC1, a brain extracellular matrix glycoprotein related to SPARC and follistatin, is expressed by rat cerebellar astrocytes following injury and during development. Brain Res. 730:95–106.

Mendis DB, Ivy GO, Brown IR. 1998. SPARC/osteonectin mRNA is induced in blood vessels following injury to the adult rat cerebral cortex. Neurochem Res. 23:1117–1123.

Mendis DB, Ivy GO, Brown IR. 2000. Induction of SC1 mRNA encoding a brain extracellular matrix glycoprotein related to SPARC following lesioning of the adult rat forebrain. Neurochem Res. 25:1637–1644.

Mendis DB, Malaval L, Brown IR. 1995. SPARC, an extracellular matrix glycoprotein containing the follistatin module, is expressed by astrocytes in synaptic enriched regions of the adult brain. Brain Res. 676:69–79.

Mendis DB, Shahin S, Gurd JW, Brown IR. 1996. SC1, a SPARC-related glycoprotein, exhibits features of an ECM component in the developing and adult brain. Brain Res. 713:53–63.

Monea S, Jordan BA, Srivastava S, DeSouza S, Ziff EB. 2006. Membrane localization of membrane type 5 matrix metalloproteinase by AMPA receptor binding protein and cleavage of cadherins. J Neurosci. 26:2300–2312.

Murayama Y, Fujita I, Kato M. 1997. Contrasting forms of synaptic plasticity in monkey inferotemporal and primary visual cortices. Neuroreport. 8:1503–1508.

Nakada M, Miyamori H, Yamashita J, Sato H. 2003. Testican 2 abrogates inhibition of membrane-type matrix metalloproteinases by other testican family proteins. Cancer Res. 63:3364–3369.

Nakada M, Yamada A, Takino T, Miyamori H, Takahashi T, Yamashita J, Sato H. 2001. Suppression of membrane-type 1 matrix metalloproteinase (MMP)-mediated MMP-2 activation and tumor invasion by testican 3 and its splicing variant gene product, N-Tes. Cancer Res. 61:8896–8902.

O'Shea J, Johansen-Berg H, Trief D, Gobel S, Rushworth MF. 2007. Functionally specific reorganization in human premotor cortex. Neuron. 54:479–490.

Oray S, Majewska A, Sur M. 2004. Dendritic spine dynamics are regulated by monocular deprivation and extracellular matrix degradation. Neuron. 44:1021–1030.

Paxinos G, Huang X, Toga A. 2000. The rhesus monkey brain in stereotaxic coodinates. San Diego (CA): Academic Press.

Pimenta AF, Zhukareva V, Barbe MF, Reinoso BS, Grimley C, Henzel W, Fischer I, Levitt P. 1995. The limbic system-associated membrane protein is an Ig superfamily member that mediates selective neuronal growth and axon targeting. Neuron. 15:287–297.

Pizzorusso T, Medini P, Berardi N, Chierzi S, Fawcett JW, Maffei L. 2002. Reactivation of ocular dominance plasticity in the adult visual cortex. Science. 298:1248–1251.

Rockland KS, Andresen J, Cowie RJ, Robinson DL. 1999. Single axon analysis of pulvinocortical connections to several visual areas in the macaque. J Comp Neurol. 406:221–250.

Sawtell NB, Frenkel MY, Philpot BD, Nakazawa K, Tonegawa S, Bear MF. 2003. NMDA receptor-dependent ocular dominance plasticity in adult visual cortex. Neuron. 38:977–985.

Schnepp A, Komp Lindgren P, Hulsmann H, Kroger S, Paulsson M, Hartmann U. 2005. Mouse testican-2. Expression, glycosylation, and effects on neurite outgrowth. J Biol Chem. 280:11274–11280.

Shintani T, Kato A, Yuasa-Kawada J, Sakuta H, Takahashi M, Suzuki R, Ohkawara T, Takahashi H, Noda M. 2004. Large-scale identification and characterization of genes with asymmetric expression patterns in the developing chick retina. J Neurobiol. 59:34–47.

Soderling JA, Reed MJ, Corsa A, Sage EH. 1997. Cloning and expression of murine SC1, a gene product homologous to SPARC. J Histochem Cytochem. 45:823–835.

Suzuki H, Yaoi T, Kawai J, Hara A, Kuwajima G, Wantanabe S. 1996. Restriction landmark cDNA scanning (RLCS): a novel cDNA display system using two-dimensional gel electrophoresis. Nucleic Acids Res. 24:289–294.

Takahata T, Hashikawa T, Higo N, Tochitani S, Yamamori T. 2008. Difference in sensory dependence of occ1/Follistatin-related protein expression between macaques and mice. J Chem Neuroanat. 35:146–157.

Takahata T, Komatsu Y, Watakabe A, Hashikawa T, Tochitani S, Yamamori T. 2006. Activity-dependent expression of occ1 in excitatory neurons is a characteristic feature of the primate visual cortex. Cereb Cortex. 16:929–940.

Tan SS, Kalloniatis M, Sturm K, Tam PP, Reese BE, Faulkner-Jones B. 1998. Separate progenitors for radial and tangential cell dispersion during development of the cerebral neocortex. Neuron. 21:295–304.

Tanigawa H, Wang Q, Fujita I. 2005. Organization of horizontal axons in the inferior temporal cortex and primary visual cortex of the macaque monkey. Cereb Cortex. 15:1887–1899.

Tochitani S, Liang F, Watakabe A, Hashikawa T, Yamamori T. 2001. The occ1 gene is preferentially expressed in the primary visual cortex in an activity-dependent manner: a pattern of gene expression related to the cytoarchitectonic area in adult macaque neocortex. Eur J Neurosci. 13:297–307.

Tremble PM, Lane TF, Sage EH, Werb Z. 1993. SPARC, a secreted protein associated with morphogenesis and tissue remodeling, induces expression of metalloproteinases in fibroblasts through a novel extracellular matrix-dependent pathway. J Cell Biol. 121:1433–1444.

Vannahme C, Gosling S, Paulsson M, Maurer P, Hartmann U. 2003. Characterization of SMOC-2, a modular extracellular calcium-binding protein. Biochem J. 373:805–814.

Vannahme C, Schubel S, Herud M, Gosling S, Hulsmann H, Paulsson M, Hartmann U, Maurer P. 1999. Molecular cloning of testican-2: defining a novel calcium-binding proteoglycan family expressed in brain. J Neurochem. 73:12–20.

Vincent AJ, Lau PW, Roskams AJ. 2008. SPARC is expressed by macroglia and microglia in the developing and mature nervous system. Dev Dyn. 237:1449–1462.

Watakabe A, Fujita H, Hayashi M, Yamamori T. 2001. Growth/differentiation factor 7 is preferentially expressed in the primary motor area of the monkey neocortex. J Neurochem. 76:1455–1464.

Wong-Riley M. 1994. Peters A, Rockland KS. 1994. Primate visual cortex: dynamic metabolic organization and plasticity revealed by cytochrome oxidase. Cereb Cortex. 10:141–200.

Wong-Riley MT, Tripathi SC, Trusk TC, Hoppe DA. 1989. Effect of retinal impulse blockage on cytochrome oxidase-rich zones in the macaque striate cortex: I. Quantitative electron-microscopic (EM) analysis of neurons. Vis Neurosci. 2:483–497.

Xu L, Tanigawa H, Fujita I. 2003. Distribution of alpha-amino-3-hydroxy-5-methyl-4-isoxazolepropionate-type glutamate receptor subunits (GluR2/3) along the ventral visual pathway in the monkey. J Comp Neurol. 456:396–407.

Yamamori T, Rockland KS. 2006. Neocortical areas, layers, connections, and gene expression. Neurosci Res. 55:11–27.

Yan Q, Sage EH. 1999. SPARC, a matricellular glycoprotein with important biological functions. J Histochem Cytochem. 47:1495–1506.